Network Experimentation for Cooperative Localization

Andrea Conti, *Senior Member, IEEE,* Matteo Guerra, Davide Dardari, *Senior Member, IEEE,* Nicolò Decarli, *Student Member, IEEE,* Moe Z. Win, *Fellow, IEEE*

***Abstract*—This paper introduces the notion of network experimentation and proposes an experimentation methodology particularly suited for cooperative wireless networks. Based on this methodology we performed extensive measurement campaigns and compare various cooperative localization techniques under a common setting. Network experiments enable (i) the quantification of cooperation benefits, (ii) the development of techniques for harnessing environmental information, and (iii) the characterization of network localization algorithms. As a case study, we consider ultrawide bandwidth cooperative location-aware networks in cluttered indoor environments and evaluate their performance based on measurements collected from network experiments.**

***Index Terms*—Network experimentation, cooperative localization, channel characterization, ultrawide bandwidth.**

I. Introduction

COOPERATION among peer nodes at the physical layer can significantly expand the capabilities of wireless networks [1]–[7]. Cooperative wireless networks play an important role in both data communication and nodes localization. Network localization and navigation is an emerging paradigm for cooperative wireless networks, in which location-awareness embraces communication [8]. The performance of such networks depends on the conditions of each link, and thus the characterization of channels associated with all links is essential for the design of cooperative wireless networks.

The design and analysis of cooperative networks require experiments specifically tailored for cooperative techniques. In particular, for cooperative location-aware networks, the following two kinds of measurements are necessary for all links:[1]

- *range measurements* for estimating the distance between each pair of nodes, and
- *waveform measurements* for estimating the range and channel state associated with each link,

both of which are used as inputs to the localization algorithms. Network experimentation based on waveform measurements enables the characterization of cooperative wireless networks for various applications. While there have been numerous works on measurements and models of wireless environments [9]–[23], they have mainly focused on point-to-point channels. To the best of the authors's knowledge, propagation experiments specifically tailored for cooperative networks are not present in the literature.

Providing location-awareness in cluttered environments is challenging primarily due to multipath, line-of-sight (LOS) blockage, and excess propagation delays through materials.[2] Ultrawide bandwidth (UWB) technology [24]–[26] can provide accurate localization in such environments [27]–[35] due to its ability to resolve multipath and penetrate obstacles [15]–[20]. UWB signals provide fine delay resolution, enabling precise time-of-arrival (TOA) measurements for range estimation between two nodes [36]–[39]. However, the accuracy and reliability of range-based localization techniques typically degrade in cluttered environments, where multipath, LOS blockage, and excess propagation delays through materials lead to positively-biased range measurements [39], [40].

As a case study, we consider the problem of network localization in realistic indoor environments, involving anchors (also referred to as beacons) and agents (also referred to as targets). In a noncooperative setting, each agent estimates the distances from neighboring anchors, which are then used as inputs to a localization algorithm for determining its own position. In a cooperative setting, each agent estimates the distances from neighboring agents in addition to those from neighboring anchors.

The localization process consists of a measurement phase where agents perform measurements with respect to anchors and others agents (in a cooperative setting), and a location update phase where agents infer their position based on prior knowledge and new measurements. The performance of localization algorithms depends mainly on two factors: (i) the geometric configuration of the network described by the positions of anchors and agents, and (ii) the quality of

Manuscript received 15 February 2011; revised 20 July 2011. This research was supported, in part, by the European Commission in the scope of the FP7 ICT project SELECT Grant no. 257544, the Italian Ministero dello Sviluppo Economico under the project WEBS, the Korean National Research Foundation under Grant NRF-2011-220-D00076, the Copernicus Fellowship, the National Science Foundation under Grant ECCS-0901034, the Office of Naval Research under Grant N00014-11-1-0397, and the MIT Institute for Soldier Nanotechnologies.

A. Conti and M. Guerra are with ENDIF and WiLAB, University of Ferrara, Italy (e-mail: a.conti@ieee.org, matteo.guerra@unife.it).

D. Dardari and N. Decarli are with WiLAB, University of Bologna, Cesena campus, Italy (e-mail: ddardari@ieee.org, nicolo.decarli@unibo.it).

M. Z. Win is with the Laboratory for Information and Decision Systems (LIDS), Massachusetts Institute of Technology, Cambridge, MA 02139 USA (email: moewin@mit.edu).

Digital Object Identifier 10.1109/JSAC.2012.120227.

[1]In principle range information can be extracted from received waveforms. However, this may require network synchronization. In our experimental setting, this is alleviated by employing radios that enable the collection of range and waveform measurements simultaneously.

[2]In these environments (e.g., inside buildings, in urban canyons, under tree canopies, and in caves), the global positioning system (GPS) is often inaccessible.

measurements affected by the propagation conditions of the environment [6], [27], [29], [39]. Localization performance can be improved significantly by selecting appropriate anchors [6], [32], [41] and mitigating the effects of unreliable range measurements [42]–[46].

In this paper, we introduce the notion of network experimentation and develop an experimentation methodology particularly suited for cooperative wireless networks. Based on this methodology, we performed extensive experiments and collected measurements associated with all of the links involved in cooperative localization. This enables the performance evaluation of various network localization algorithms under a common setting. The key contributions of the paper can be summarized as follows:

- development of experimentation methodology for the characterization of cooperative wireless networks in realistic environments;
- establishment of database with range and waveform measurements for cooperative wireless channels; and
- characterization of range errors and evaluation of network localization algorithms accounting for various LOS and non-line-of-sight (NLOS) conditions.

The remainder of the paper is organized as follows. The experimentation methodology for cooperative location-aware networks is presented in Section II. In Section III, we present the results of the measurement campaign and devise range error model. Section IV describes a technique for range error mitigation and position refinement. In Section V, we present a case study on UWB indoor cooperative localization. Finally, conclusions are given in Section VI.

II. Network Experimentation Methodology

We now describe the network experiments tailored specifically for design and analysis of cooperative location-aware networks under a common set of measurements.[3] The performance of such networks is dominated by the behavior of range errors. Range estimates based on TOA measurements are typically corrupted by thermal noise, multipath fading, direct path (DP) blockage, and DP excess delay [39]. A range measurement is referred to as a DP measurement if it is obtained from a signal traveling along a straight line between the two nodes. A measurement is non-DP if the DP signal is completely obstructed (i.e., DP blockage) and the first signal to arrive at the receiver comes from reflected paths only. Another source of error is the DP excess delay caused by the propagation of a partially obstructed DP component that travels through different obstacles (e.g., furniture and walls).[4] An important observation to be made is that DP blockage and DP excess delay have the same effects on range measurements: they both add a positive bias to the true distance between the nodes. These measurements are referred to as NLOS measurements. A LOS measurement occurs when the signal travels along an unobstructed DP.

[3]While the experiments were performed in indoor environments, the methodology can be also applied to outdoor scenarios.

[4]Given a homogeneous material with relative electrical permittivity ϵ_r, the speed of the electromagnetic wave travelling inside materials is slowed down by a factor $\sqrt{\epsilon_r}$ with respect to the speed of light c. Hence the extra delay introduced by a wall of thickness d_W is $\Delta \simeq (\sqrt{\epsilon_r} - 1)\, d_W/c$.

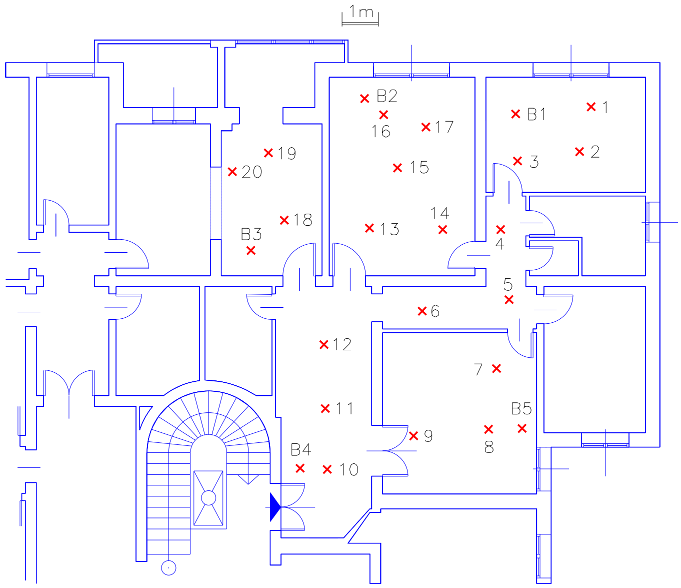

Fig. 1. A typical apartment in Bologna, Italy, serving as the network experimentation environment.

The geometry of the network, the propagation conditions of the links, and types of obstacles, all of which affect the performance of cooperative wireless networks, are described in the following.

A. Network Geometry

We consider wireless networks in indoor environments with a geometric configuration consisting of N_b anchors deployed in known positions to determine the unknown positions of N_a agents. In particular, we chose a set of positions for anchors and agents, and performed simultaneous range and waveform measurements for all possible links between pairs of nodes.[5] An extensive measurement campaign was carried out in a typical apartment with furniture and concrete walls with thickness of 15 and 30 cm (Fig. 1).

We consider $N_p = 25$ nodes positions. All nodes can be treated as anchors or agents; nevertheless $N_b = 5$ positions (labeled B1-B5) have been considered for anchors and $N_a = 20$ for agents (numbered 1-20) to compare noncooperative and cooperative networks. Range and waveform measurements for each pair of anchor and agent were made for a noncooperative setting (i.e., 5×20 links). In addition, measurements between each pair of agents were also made for a cooperative setting (i.e., additional $\binom{20}{2}$ links). A total of 1500 measurements were collected for each pair of nodes in both settings.

B. Links Characterization

The characterization of cooperative wireless networks requires measurements for all links between pairs of nodes (agent and anchor or two cooperating agents). Such measurements were performed using UWB radios operating in the $3.2 - 7.4$ GHz band. These commercial radios can provide (i) range measurements through TOA estimation based on

[5]In general, the selection of nodes positions can be based on a grid or by choosing key positions in the environment (e.g., specific places in a room or in a corridor).

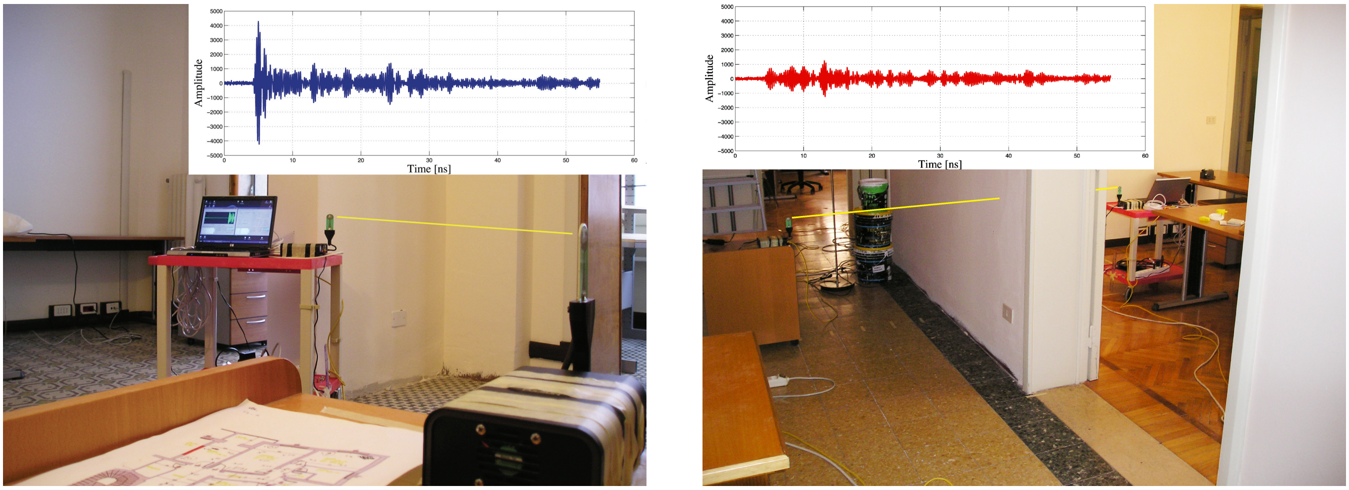

(a) LOS condition.

(b) NLOS condition.

Fig. 2. Views of measurement setup and corresponding received waveforms in the experimentation environment.

thresholding techniques,[6] and (ii) samples of received signal waveforms. Waveform measurements for each link can be thought of as channel impulse response owing to the use of signals with extremely large bandwidth. Measurement setup examples for LOS and NLOS conditions are shown in Fig. 2(a) and Fig. 2(b), respectively.

A pair of nodes can be in LOS or NLOS condition depending on their relative positions in the environment. Figure 2 also shows waveform measurements collected, representing typical channel pulse responses in LOS and NLOS conditions in the network experimentation environment of Fig. 1. It can be seen from the figures that LOS and NLOS conditions give rise to different behaviors of waveform measurements. The presence of multipath, typical of indoor environments, is also noticeable in both conditions. The knowledge of the NLOS condition can be exploited to mitigate ranging errors to significantly improve the performance of the localization algorithms.

Let $d_{i,j}$ denotes the Euclidean distance between two nodes (i.e., an agent and a reference node, which can be either an anchor or a cooperative agent) in positions $\mathbf{p}_i$ and $\mathbf{p}_j$, respectively. Note that UWB radios provide ranging accuracy on the order of a few centimeters, and thus the true distance between each pair of nodes must be known with an accuracy better than a centimeter. On the other hand, determining the true distance between two nodes with obstacles (e.g., walls) in between can be difficult even using laser-based ranging devices. This difficulty is alleviated by using a 3D computer-aided design software.

C. Obstacles Characterization

To characterize the bias of ranging errors due to obstacles, additional range measurements were collected in the environment. The transmitting and receiving nodes were placed in several positions, in addition to those in Fig. 1, such that one or two walls with different thicknesses were present between the two nodes.[7] Range measurements were collected using UWB radios located in five sets of short distances (i.e., 20, 40, 60, 80, and 100 cm from both sides of the walls) to isolate the effects of excess delay from those of multipath. A view of the measurement setup is given in Fig. 2(b). By using the collected range measurements ensemble (5×1500 measurements), the mean (bias) and standard deviation of range errors were calculated respectively as: 16.4 cm and 3.7 cm for one wall with thickness $d_{\mathrm{W}} = 15.5$ cm; 29.5 cm and 3.2 cm for one wall with $d_{\mathrm{W}} = 30.0$ cm; and 45.2 cm and 3.0 cm for two walls with total $d_{\mathrm{W}} = 15.5 + 30.0$ cm. As can be noted, the bias appears to increase with the thickness of the wall. The values of the standard deviation suggest that the range errors are dominated by the effects of excess delay rather than those of multipath and thermal noise. From the ensemble of measurements we observe that $\Delta \simeq d_{\mathrm{W}}/c$.[8]

In the following sections, the measurements from our network experiments will be used to model range errors, to quantify the benefit of harnessing environmental information, and to compare various cooperative localization techniques under a common setting.

III. Range Error Model

Understanding the behavior of range errors is essential for the development of cooperative localization techniques. In the following, range model based on measurements in Section II-B and range error bias model based on measurements in Section II-C will be developed.

We start by categorizing these link measurements in Section II-B in terms of the channel state (e.g., the state $\mathcal{H}_i$ indicates i walls between a pair of nodes with $i = 0, 1, ..., 4$). Figure 3 shows the range error bias (i.e., average range error over 1500 measurements) for each link as a function of the true distance, in LOS ($\mathcal{H}_0$) and NLOS ($\mathcal{H}_1$, $\mathcal{H}_2$, $\mathcal{H}_3$, and $\mathcal{H}_4$) conditions. Note that the bias depends strongly on the total thickness of the walls. Range measurements described in Section II-B also show that the range $r_{i,j}$ between the pair of nodes i and j, in

[6] A survey on ranging techniques and performance limits is given in [39].

[7] Preliminary measurements were reported in [47], here these measurements are used for evaluating the performance of network localization.

[8] This correspond to $\epsilon_{\mathrm{r}} \simeq 4$. The value of ϵ_{r}, which depends on the material of the wall, is confirmed by a similar result obtained in [48].

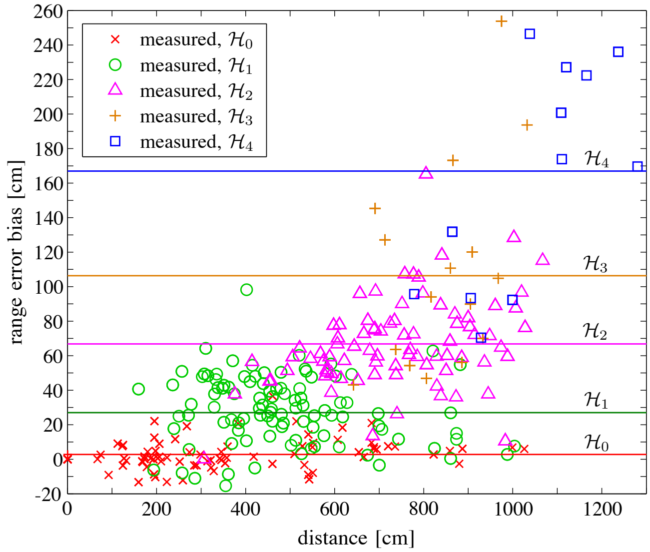

Fig. 3. Range error bias as a function of distance for nodes pairs in LOS or NLOS conditions.

both LOS and NLOS conditions, can be modeled as

$$r_{i,j} = d_{i,j} + b_{i,j} + \epsilon_{i,j} \tag{1}$$

where $d_{i,j}$ is the true distance and $b_{i,j}$ is the range error bias. The quantity $\epsilon_{i,j}$ is modeled as a zero mean random variable (RV), independent of $b_{i,j}$, with variance $\sigma^2_{i,j}$ [47]. It can be observed from the measurements that $b_{i,j}$ and $\sigma^2_{i,j}$ depend on the obstacles (e.g., the number of walls) between nodes i and j. Equation (1) was also used in [32], [40], where $b_{i,j}$ and $\sigma^2_{i,j}$ were modeled as a function of true distance.

We expect the bias $b_{i,j}$ to vary more in a cluttered environment (with many walls, machines, and furniture such as in a typical office building) than in an open environment.

When the environmental information (e.g., the number of walls and the excess delay) is available, $b_{i,j}$ in (1) can be modeled as a function of the excess delay, namely

$$b_{i,j} = c \sum_{k=1}^{N_{\rm w}(i,j)} n_k^{(i,j)} \Delta_k \tag{2}$$

where c is the speed of light, $N_{\rm w}(i,j)$ is the number of different extra delay values, and $n_k^{(i,j)}$ is the number of walls that result in the same extra delay value Δ_k (e.g., the number of walls with the same material and thickness). We refer to this model as wall extra delay (WED) bias model. The total number of walls between the two nodes is

$$n^{(i,j)} = \sum_{k=1}^{N_{\rm w}(i,j)} n_k^{(i,j)} . \tag{3}$$

When every wall in the scenario has the same thickness and composition (i.e., $\Delta_k = \Delta$ for each k), (2) simplifies to

$$b_{i,j} = c\, n^{(i,j)} \Delta . \tag{4}$$

We will show in Section IV that the WED bias model can be used to mitigate range errors, resulting in significant improvement of localization performance.

IV. Harnessing Environmental Information

The environmental information can be harnessed to mitigate range errors, and thus improving localization accuracy. Such information can be obtained from environmental knowledge or by processing the received waveforms using channel state identification techniques. These two cases will be referred to as WED bias model with environmental information (known number of walls) and WED bias model with channel state identification (estimated number of walls), respectively. Regardless of the particular localization algorithm, the three-step procedure described in Algorithm 1 may be adopted.

Algorithm 1 Range error mitigation and position refinement

1. *Initial position estimate:* obtain an initial position estimate $\hat{\mathbf{p}}^{(1)}$ based on the range measurements;
2. *Range error mitigation:* mitigate bias of the range error from measurements according to the bias model and the initial position estimate $\hat{\mathbf{p}}^{(1)}$;
3. *Position refinement:* update the position estimate $\hat{\mathbf{p}}^{(2)}$ with the corrected range values.

A. Channel State Identification Techniques

A classical approach to channel state identification involves binary hypothesis testing between LOS and NLOS conditions (see, e.g., [49], [50]). Localization techniques based on binary channel state (i.e., LOS or NLOS) can be further improved by considering a larger number of channel states (i.e., M-ary hypothesis), which accounts for the number of obstacles between each pair of nodes. In particular, we consider maximum a posteriori probability (MAP) decision rule as

$$\mathcal{D} = \arg\max_{\mathcal{H}\in\mathcal{C}} p(\boldsymbol{\gamma}|\mathcal{H})\, \mathbb{P}\{\mathcal{H}\} \tag{5}$$

where $\boldsymbol{\gamma} = \{\gamma_1, \gamma_2, \dots, \gamma_{N_{\rm f}}\}$ is a set of $N_{\rm f}$ features extracted from a received waveform, $\mathcal{C}$ is the set of possible channel states, $p(\boldsymbol{\gamma}|\mathcal{H}_i)$ is the joint probability distribution function (PDF) of features conditioned on $\mathcal{H}_i$, and $\mathbb{P}\{\mathcal{H}_i\}$ is the *a priori* probability that there are i walls between two nodes.[9]

A key step in designing the MAP decision rule (5) is choosing the appropriate set of features $\boldsymbol{\gamma}$ extracted from received waveforms. Examples of features include: (i) the root mean square (RMS) delay spread $\tau_{\rm RMS}$; (ii) the kurtosis κ; and (iii) the maximum amplitude $\upsilon_{\rm MAX}$. In LOS conditions, the first path in the received signal is typically the strongest. Compared to NLOS, LOS propagation typically gives rise to smaller delay spread and a larger kurtosis [45].

Measurements described in Section II-B also show that each feature can be modeled as a log-normal RV, with parameters that depend on the environment. In this case, the PDF for a generic feature γ can be written as [45], [51]

$$p(\gamma|\mathcal{H}_i) = \frac{1}{\gamma\sqrt{2\pi\sigma_i^2}} e^{-\frac{(\ln\gamma-\mu_i)^2}{2\sigma_i^2}} \tag{6}$$

where μ_i and σ_i are the parameters for channel state $\mathcal{H}_i$, and $\ln(\cdot)$ indicates the natural logarithm. The parameters μ_i and σ_i

[9]When more than one feature is extracted from the waveform, it is often difficult to determine the joint PDF. This can be alleviated by considering all the features γ_i as independent RVs.

TABLE I
PARAMETERS μ_i AND σ_i (MEASURED IN [ns] FOR τ_{RMS} AND IN [ADC bins] FOR υ_{MAX}) CORRESPONDING TO CHANNEL STATE $\mathcal{H}_i$.

	τ_{RMS}		κ		υ_{MAX}	
$\mathcal{H}_i$	μ_i	σ_i	μ_i	σ_i	μ_i	σ_i
$\mathcal{H}_0$	1.24	0.24	2.97	0.40	8.66	0.43
$\mathcal{H}_1$	1.43	0.29	3.01	0.34	8.00	0.50
$\mathcal{H}_2$	2.05	0.39	2.82	0.40	7.00	0.64
$\mathcal{H}_3$	2.47	0.24	2.50	0.37	6.20	0.45
$\mathcal{H}_4$	2.68	0.16	2.34	0.33	5.90	0.33

for features τ_{RMS}, κ, and υ_{MAX} have been determined from the measured waveforms, and the results are reported in Table I. Figure 4 shows the cumulative distribution functions (CDFs) of features τ_{RMS}, κ, and υ_{MAX} for each channel state $\mathcal{H}_i$ ($i = 0, 1, \ldots, 4$). The figure also shows the CDFs of log-normal distributions using parameters μ_i and σ_i from Table I. Note that the log-normal distribution fits the CDF of features τ_{RMS} for all channel states $\mathcal{H}_i$ except for $\mathcal{H}_4$, which occur less frequently in our network experiments as shown in Sec. IV-B. Similar fit can be seen for the CDF of features κ and υ_{MAX} for all channel states $\mathcal{H}_i$ except for $\mathcal{H}_2$ and $\mathcal{H}_0$, respectively.

B. Channel State Identification Performance

We now apply the MAP decision rule to waveform measurements described in Section II-B for identification of channel states in the set $\mathcal{C} = \{\mathcal{H}_0, \mathcal{H}_1, \ldots, \mathcal{H}_4\}$. Table II shows the $\widehat{p}_{i,j}$, namely the estimate of $\mathbb{P}\{\mathcal{D} = \mathcal{H}_i | \mathcal{H}_j\}$ for $i, j = 0, 1, \ldots, 4$, describing the probability of deciding $\mathcal{D} = \mathcal{H}_i$ (i walls) when the condition $\mathcal{H}_j$ (j walls) is true. In particular, different features sets $\gamma_{\mathrm{a}} = \{\tau_{\mathrm{RMS}}\}$, $\gamma_{\mathrm{b}} = \{\kappa\}$, $\gamma_{\mathrm{c}} = \{\upsilon_{\mathrm{MAX}}\}$, and $\gamma_{\mathrm{joint}} = \{\tau_{\mathrm{RMS}}, \kappa, \upsilon_{\mathrm{MAX}}\}$ are used with MAP decision rule (5). Note that the use of joint features improves the channel state identification compared to a single feature, as expected. The correct identification probability for a features set γ can be estimated as

$$\widehat{p}_{\mathrm{corr}}(\gamma) = \sum_{i=0}^{4} \widehat{p}_{i,i}\, \mathbb{P}\{\mathcal{H}_i\} \ . \tag{7}$$

In our network experimentation, we have $\mathbb{P}\{\mathcal{H}_0\} = 0.286$, $\mathbb{P}\{\mathcal{H}_1\} = 0.343$, $\mathbb{P}\{\mathcal{H}_2\} = 0.274$, $\mathbb{P}\{\mathcal{H}_3\} = 0.058$ and $\mathbb{P}\{\mathcal{H}_4\} = 0.039$. Using these together with Table II, we obtain $\widehat{p}_{\mathrm{corr}}(\gamma_{\mathrm{a}}) = 0.91$, $\widehat{p}_{\mathrm{corr}}(\gamma_{\mathrm{b}}) = 0.85$, $\widehat{p}_{\mathrm{corr}}(\gamma_{\mathrm{c}}) = 0.91$, and $\widehat{p}_{\mathrm{corr}}(\gamma_{\mathrm{joint}}) = 0.92$.

V. CASE STUDY: COOPERATIVE LOCALIZATION-AWARE NETWORKS

We now analyze and compare the performance of various localization techniques under a common set of measurements collected from our network experiments in the environment of Fig. 1. In particular, we consider sum-product algorithm over a wireless network (SPAWN), which aims to infer agents positions based on measurements among nodes.[10] Results are given for SPAWN with and without range error mitigation techniques. In the case of range error mitigation, both WED bias model with environmental information and WED bias model with channel state identification based on MAP decision are considered. In the following, localization performance metrics are described and evaluated for noncooperative and cooperative settings.

[10]This algorithm, based on Bayesian inference, relies on network factor graph (FG) and network message passing [52].

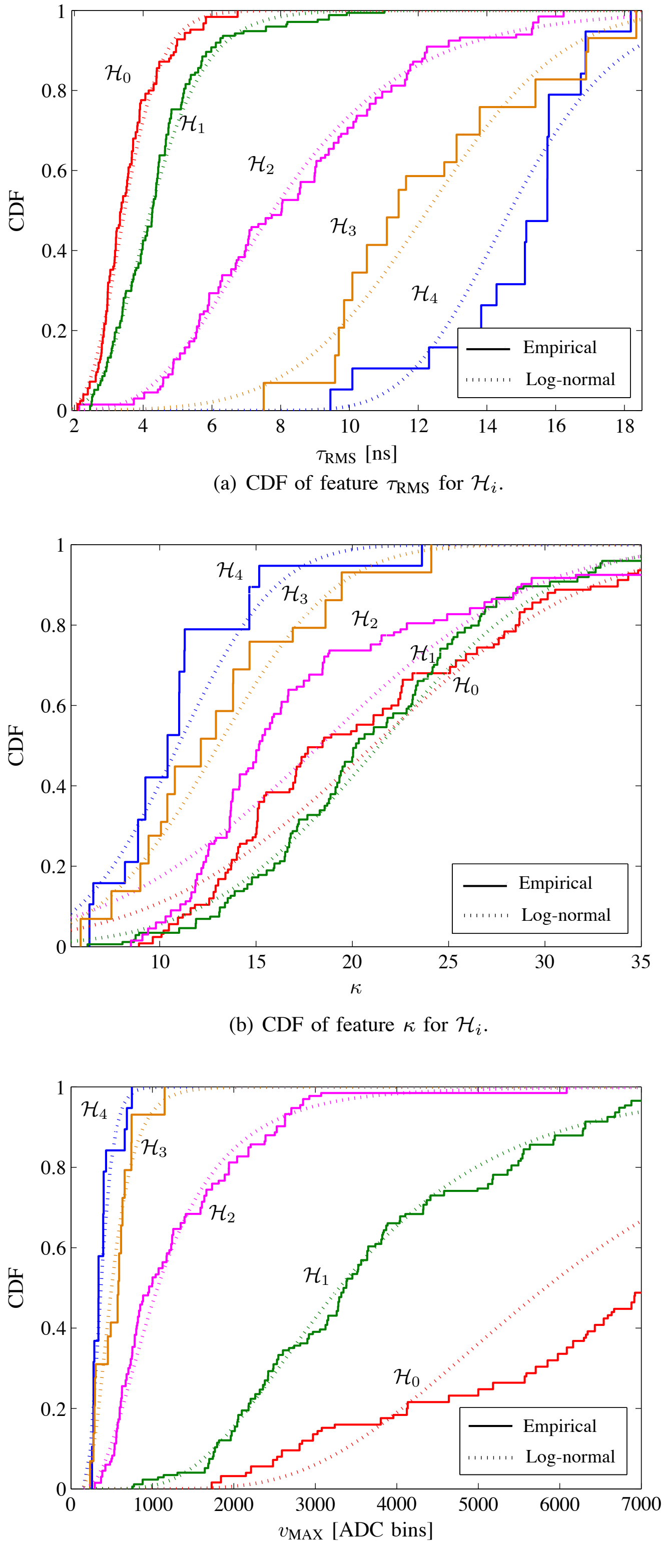

(a) CDF of feature τ_{RMS} for $\mathcal{H}_i$.

(b) CDF of feature κ for $\mathcal{H}_i$.

(c) CDF of feature υ_{MAX} for $\mathcal{H}_i$.

Fig. 4. Empirical CDF of features extracted from measured waveforms and CDF of the log-normal distributions with parameters from Table I for LOS ($\mathcal{H}_0$) and NLOS ($\mathcal{H}_i$ with $i = 1, 2, 3,$ and 4 walls) conditions.

TABLE II
$\widehat{p}_{i,j}$ FOR $i,j=0,1,\ldots,4$ USING FEATURES SETS $\boldsymbol{\gamma}_{\mathrm{a}}$ (FIRST ROW), $\boldsymbol{\gamma}_{\mathrm{b}}$ (SECOND ROW), $\boldsymbol{\gamma}_{\mathrm{c}}$ (THIRD ROW), AND $\boldsymbol{\gamma}_{\mathrm{joint}}$ (FOURTH ROW).

$\mathcal{H}$ \ $\mathcal{D}$	$\mathcal{H}_0$	$\mathcal{H}_1$	$\mathcal{H}_2$	$\mathcal{H}_3$	$\mathcal{H}_4$
$\mathcal{H}_0$	0.958	0.042	0	0	0
	0.790	0.111	0.021	0.042	0.035
	0.958	0.042	0	0	0
	0.958	0.042	0	0	0
$\mathcal{H}_1$	0.057	0.896	0.034	0.011	0
	0.017	0.919	0.023	0.017	0.023
	0.034	0.919	0.034	0.011	0
	0.046	0.901	0.040	0.011	0
$\mathcal{H}_2$	0	0.044	0.889	0.051	0.014
	0.014	0.066	0.823	0.066	0.029
	0	0.051	0.882	0.066	0
	0	0.036	0.904	0.051	0.007
$\mathcal{H}_3$	0	0	0	0.931	0.069
	0	0.034	0	0.931	0.034
	0	0	0	0.965	0.034
	0	0	0	0.965	0.034
$\mathcal{H}_4$	0	0	0	0.176	0.823
	0	0.058	0.058	0	0.882
	0	0	0	0.176	0.823
	0	0	0	0.176	0.823

A. Performance Metrics

We consider localization error and localization error outage (LEO), since these metrics provide insights into local and global behavior of localization techniques, respectively. For a given scenario (e.g., the number of anchors N_{b} and agents N_{a}, the network setting, and the environment), the localization error is defined as the Euclidean distance between the estimated position $\hat{\mathbf{p}}$ and the true position $\mathbf{p}$, namely

$$e(\mathbf{p}) = ||\hat{\mathbf{p}} - \mathbf{p}|| \,. \tag{8}$$

The LEO is given in terms of the outage probability (OP), based on the localization error, as[11]

$$\begin{aligned} P_{\mathrm{o}} &= \mathbb{P}\{e(\mathbf{p}) > e_{\mathrm{th}}\} \\ &= \mathbb{E}\left\{\mathbb{1}_{(e_{\mathrm{th}},+\infty)}\left(||\hat{\mathbf{p}} - \mathbf{p}||\right)\right\} \end{aligned} \tag{9}$$

where e_{th} is the target (i.e., the maximum allowable) localization error, and $\mathbb{1}_{\mathcal{A}}(x) = 1$ when $x \in \mathcal{A}$ and 0 otherwise. Here the statistical expectation $\mathbb{E}\{\cdot\}$ is over the ensemble of all possible spatial positions and temporal instants.

B. Performance of Noncooperative Localization

For noncooperative localization, two cases with $N_{\mathrm{b}} = 3$ and $N_{\mathrm{b}} = 5$ anchors are considered. In the case of $N_{\mathrm{b}} = 3$ anchors, there are $\binom{5}{3}$ possible configurations over positions (B1-B5), among which three anchors in the positions set $\mathcal{B}_3$ ={B1, B3, B5} are selected. This choice is guided by corresponding mean (22.9 cm) and standard deviation (5.0 cm) of the position error bound (PEB) over all agents positions.[12] In the case of $N_{\mathrm{b}} = 5$ anchors, the positions set $\mathcal{B}_5$ ={B1, B2, B3, B4, B5} leads to mean (13.6 cm) and standard deviation (5.2 cm) of the PEB over all agents positions.[13]

In Table III, the localization error is evaluated for each position in the environment (ID 1-20 in Fig. 1). Localization errors without range error mitigation for $N_{\mathrm{b}} = 5$ anchors (in positions set $\mathcal{B}_5$) and that for $N_{\mathrm{b}} = 3$ anchors (in positions set $\mathcal{B}_3$) are reported in columns A and B, respectively. Comparing columns A and B shows that using a larger number of anchors does not necessarily lead to a better localization accuracy. Next, we examine the effects of range error mitigation techniques using the WED bias model both with environmental information and with channel state identification based on MAP decision and features set $\boldsymbol{\gamma}_{\mathrm{joint}}$. Localization errors with range error mitigation using the WED bias model with environmental information are reported in Table III columns C and D for $N_{\mathrm{b}} = 5$ anchors (in positions set $\mathcal{B}_5$) and $N_{\mathrm{b}} = 3$ anchors (in positions set $\mathcal{B}_3$), respectively. Comparing columns A and C or columns B and D shows that range error mitigation techniques can significantly reduce the localization error. Localization errors with range error mitigation using the WED bias model with channel state identification are reported in columns E and F for $N_{\mathrm{b}} = 5$ anchors (in positions set $\mathcal{B}_5$) and $N_{\mathrm{b}} = 3$ anchors (in positions set $\mathcal{B}_3$), respectively. Comparing columns C and E or columns D and F shows that range error mitigation techniques using the WED bias model with known and inferred number of walls result in similar localization performance.

Figure 5 shows the noncooperative LEO as a function of the target localization error for $N_{\mathrm{b}} = 5$ and $N_{\mathrm{b}} = 3$ anchors with and without range error mitigation. The benefit of range error mitigation is evident from this figure. For example, with $N_{\mathrm{b}} = 3$ anchors and no range error mitigation, the LEO is 0.1 with e_{th} about 69.3 cm, meaning that the localization error is no greater than 69.3 cm in 90% of cases. For range error mitigation using the WED bias model with environmental information, the LEO is 0.1 with e_{th} about 37.4 cm.

C. Performance of Cooperative Localization

We now evaluate the performance of cooperative localization techniques. The effectiveness of cooperation is quantified in terms of localization error and LEO for the cases with and without range error mitigation.

In Table IV, the localization error is evaluated for each position in the environment (ID 1-20 in Fig. 1). Various cooperative settings are considered for $N_{\mathrm{b}} = 3$ anchors (in positions set $\mathcal{B}_3$) with and without range error mitigation. Specifically, we consider each agent cooperating with another agent in a position either 6 or 15. We also consider each agent cooperating with two other agents in positions 6 and 15. Localization errors are reported for the case of single cooperating agent without range error mitigation and those with range error mitigation using the WED bias model both with environmental information and with channel state identification based on MAP decision and features set $\boldsymbol{\gamma}_{\mathrm{joint}}$. Specifically, columns

[11]The OP is a well known concept for performance evaluation of wireless communication systems (see, e.g., [53]). Similarity with location-aware networks is in evaluating the probability that the quality of service falls below a given target.

[12]These values are based on [32] with no range error bias. The fundamental limits (lower bound) on the accuracy, based on the received waveforms, of any localization methods were derived in terms of squared PEB for a noncooperative setting in [28] and for a cooperative setting in [6].

[13]In the case of $N_{\mathrm{b}} = 4$ anchors, there are $\binom{5}{4}$ possible configurations over positions (B1-B5) and we verified that the PEB values for these configurations are close to each other. For example, the anchors in positions set $\mathcal{B}_4$ ={B2, B3, B4, B5} leads to mean (15.52 cm) and standard deviation (6.28 cm) of the PEB over all agents positions.

TABLE III
NONCOOPERATIVE LOCALIZATION ERROR $e(\mathbf{p})$ [cm]
FOR EACH NODE POSITION (ID) IN VARIOUS SETTINGS A-F.

ID	A	B	C	D	E	F
1	28.1	34.9	28.9	32.5	55.4	38.8
2	79.0	47.1	10.8	8.4	8.7	35.7
3	85.9	23.3	5.3	6.8	13.4	14.0
4	78.5	67.3	18.4	29.8	18.4	29.8
5	37.9	50.8	40.8	37.4	42.5	32.6
6	16.5	62.7	30.1	30.6	38.9	39.3
7	60.4	67.9	19.7	24.5	37.3	27.9
8	37.8	77.0	15.3	9.4	7.1	8.8
9	57.8	56.0	14.7	9.1	14.7	22.3
10	46.8	48.1	18.5	28.4	8.0	5.99
11	57.7	58.3	22.6	20.9	13.0	30.9
12	35.4	36.8	13.8	1.2	10.7	50.9
13	37.6	35.7	13.8	12.4	26.1	85.8
14	26.7	14.4	7.6	29.9	11.3	16.8
15	55.9	31.4	23.2	21.0	25.9	37.3
16	14.4	52.5	5.3	15.1	25.9	31.2
17	20.0	70.7	17.4	23.7	16.2	21.9
18	60.1	59.8	29.1	30.0	18.7	35.7
19	74.8	51.1	26.2	35.6	19.7	29.7
20	39.8	39.1	47.8	52.5	28.5	46.8
Mean	47.6	49.3	20.5	23.0	22.0	32.1
StD	21.6	16.6	11.1	12.7	13.1	17.2
Span	71.5	62.6	42.5	51.3	48.3	79.8

A: $N_{\mathrm{b}} = 5$ without range error mitigation
B: $N_{\mathrm{b}} = 3$ without range error mitigation
C: $N_{\mathrm{b}} = 5$ with range error mitigation (WED env. information)
D: $N_{\mathrm{b}} = 3$ with range error mitigation (WED env. information)
E: $N_{\mathrm{b}} = 5$ with range error mitigation (WED MAP decision)
F: $N_{\mathrm{b}} = 3$ with range error mitigation (WED MAP decision)

TABLE IV
COOPERATIVE LOCALIZATION ERROR $e(\mathbf{p})$ [cm]
FOR EACH NODE POSITION (ID) WITH $N_{\mathrm{B}} = 3$ IN VARIOUS SETTINGS A-I.

ID	A	B	C	D	E	F	G	H	I
1	31.5	29.1	38.8	33.1	27.8	38.9	17.4	12.3	41.5
2	52.9	8.1	35.7	46.7	4.6	31.6	73.7	8.2	7.5
3	18.1	6.0	14.0	24.3	6.9	14.6	40.8	6.4	11.5
4	27.7	24.0	29.8	37.5	22.1	28.8	38.5	16.5	20.1
5	60.3	38.3	32.6	20.0	39.2	33.2	33.9	36.8	36.3
6	-	-	-	29.1	37.1	38.0	-	-	-
7	36.5	17.4	27.9	37.4	23.7	24.0	27.9	15.5	39.6
8	52.6	10.5	8.7	72.9	10.6	9.2	22.7	11.8	10.2
9	51.9	9.5	22.3	41.1	8.9	17.3	59.4	8.7	21.5
10	45.9	28.7	6.0	39.1	21.9	2.2	32.1	34.9	13.0
11	55.2	20.9	30.9	20.5	16.7	27.4	21.9	16.6	16.9
12	7.2	2.3	50.9	37.8	3.2	43.0	4.8	2.1	10.1
13	16.0	13.4	85.7	91.9	12.4	85.7	21.3	13.8	24.0
14	8.0	30.6	16.7	67.1	27.6	16.9	39.2	29.3	6.3
15	22.3	21.7	37.3	-	-	-	-	-	-
16	46.3	17.2	31.2	54.5	11.8	30.9	16.1	14.7	24.6
17	65.0	26.3	21.9	40.3	29.2	21.4	42.1	32.0	17.4
18	59.8	27.0	35.7	39.1	30.7	31.2	57.8	25.9	7.6
19	57.6	38.1	29.7	53.4	28.8	35.6	78.7	61.7	30.2
20	51.1	51.3	46.8	30.9	47.2	44.1	35.4	45.6	24.9
Mean	40.3	22.1	31.7	43.0	21.6	30.2	36.8	21.8	20.2
StD	18.7	12.6	17.6	18.4	12.5	17.5	20.0	5.6	11.5
Span	57.8	49.0	79.7	71.9	44.0	83.5	71.8	59.6	35.2

A: coop. agent 6, no range error mitigation
B: coop. agent 6, range error mitigation (WED env. information)
C: coop. agent 6, range error mitigation (WED MAP decision)
D: coop. agent 15, no range error mitigation
E: coop. agent 15, range error mitigation (WED env. information)
F: coop. agent 15, range error mitigation (WED MAP decision)
G: coop. agents 6 and 15, no range error mitigation
H: coop. agents 6 and 15, range error mitigation (WED env. information)
I: coop. agents 6 and 15, range error mitigation (WED MAP decision)

A, B, and C are for the case when cooperating agent is in position 6, and columns D, E, and F are for the case when the cooperating agent is in position 15. By comparing columns A with B and C or columns D with E and F shows that, similar to noncooperative setting, range error mitigation techniques can significantly reduce the localization error for cooperative localization. Localization errors for the case of two cooperating agents in positions 6 and 15 are reported in columns G, H, and I. Comparing columns G, H, and I with A, B, and C, or D, E, and F, reveals that more cooperative agents does not always improve the localization performance.

Figure 6 shows the cooperative LEO as a function of the target localization error for $N_{\mathrm{b}} = 3$ anchors with and without range error mitigation. Similar to noncooperative setting, the benefit of range error mitigation for cooperative localization is evident. For example, with $N_{\mathrm{b}} = 3$ anchors and no range error mitigation, the cooperative LEO for two cooperating agents is 0.1 with e_{th} about 59.4 cm, meaning that the localization error is no greater than 59.4 cm in 90% of cases. For range error mitigation using the WED bias model with environmental information, the cooperative LEO for two cooperating agents is 0.1 with e_{th} about 36.4 cm.

We now compare the performance of noncooperative and cooperative localization reported in Tables III and IV, respectively. It can be observed that cooperation does not always improve the localization performance. This behavior can be attributed to the fact that the link between cooperating agents can be subjected to large measurements uncertainty due to propagation conditions.

VI. CONCLUSION

We introduced the notion of network experimentation and put forth an experimentation methodology particularly suited for cooperative wireless networks. Based on this methodology we performed extensive measurement campaigns, including ranges and waveforms measurements, for network localization. The collected measurements enable the modeling of range errors for various propagation conditions, the development of channel state identification and range error mitigation techniques, as well as the comparison of various cooperative and noncooperative localization techniques under a common setting. The results provide insights into how and when cooperative techniques and environmental information can be harnessed to improve the performance of location-aware networks. It is shown that range error mitigation techniques can significantly improve the performance of network localization. The choice of the appropriate cooperating agent depends typically on the inter-agent link conditions and range error mitigation techniques. In several cases, most of the cooperation benefits can be reaped with a single suitably chosen cooperating agent. This paper demonstrates that network experiments are essential for design and analysis of cooperative wireless networks.

ACKNOWLEDGMENTS

The authors wish to thank O. Andrisano and M. Chiani for hosting the experimental campaigns at the University of Bologna; and R. Cohen, A. Rabbachin, Y. Shen, and S. Mazuelas for helpful discussions.

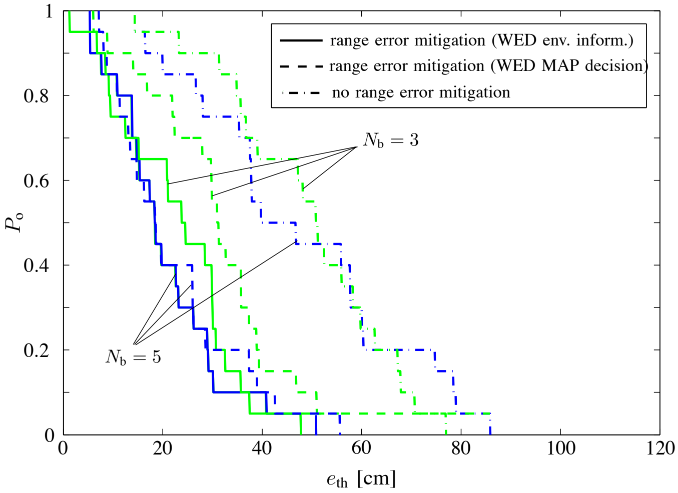

Fig. 5. Noncooperative LEO as a function of e_{th} [cm] with different range error mitigation techniques. The dark blue and light green curves show the LEO for $N_b = 5$ and $N_b = 3$ anchors, respectively.

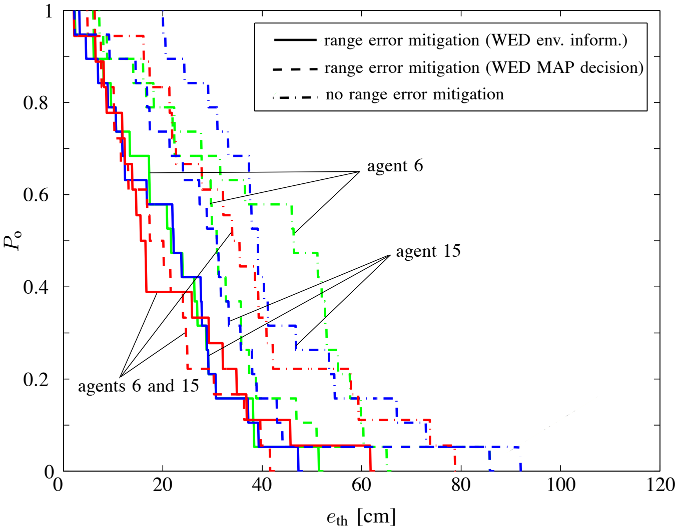

Fig. 6. Cooperative LEO as a function of e_{th} [cm] for $N_b = 3$ anchors and with different range error mitigation techniques. The light green and dark blue curves show the LEO with cooperating agent 6 and 15, respectively. The red curves show the LEO with two cooperating agents 6 and 15.

REFERENCES

[1] A. Sendonaris, E. Erkip, and B. Aazhang, "User cooperation diversity – Part I: System description," *IEEE Trans. Commun.*, vol. 51, no. 11, pp. 1927–1938, Nov. 2003.

[2] J. N. Laneman, D. N. C. Tse, and G. W. Wornell, "Cooperative diversity in wireless networks: Efficient protocols and outage behavior," *IEEE Trans. Inf. Theory*, vol. 50, no. 12, pp. 3062–3080, Dec. 2004.

[3] A. Bletsas, H. Shin, and M. Z. Win, "Cooperative communications with outage-optimal opportunistic relaying," *IEEE Trans. Wireless Commun.*, vol. 6, no. 9, pp. 3450–3460, Sep. 2007.

[4] M. Dohler, "*Virtual Antenna Arrays*," Ph.D. dissertation, Centre for Telecommunications Research, Department of Electrical Engineering, Kings College London, London, UK, Dec. 2003, thesis advisor: Professor A. Hamid Aghvami.

[5] M. Dohler, A. Gkelias, and A. Aghvami, "Capacity of distributed PHY-layer sensor networks," *IEEE Trans. Veh. Technol.*, vol. 55, no. 2, pp. 622 – 639, Mar. 2006.

[6] Y. Shen, H. Wymeersch, and M. Z. Win, "Fundamental limits of wideband localization – Part II: Cooperative networks," *IEEE Trans. Inf. Theory*, vol. 56, no. 10, pp. 4981–5000, Oct. 2010. [Online]. Available: http://arxiv.org/abs/1006.0890v1

[7] Y. Shen, S. Mazuelas, and M. Z. Win, "Cooperative network navigation: Fundamental limit and its geometrical interpretation," *IEEE J. Sel. Areas Commun.*, vol. 30, 2012, to appear.

[8] M. Z. Win, A. Conti, S. Mazuelas, Y. Shen, W. M. Gifford, D. Dardari, and M. Chiani, "Network localization and navigation via cooperation," *IEEE Commun. Mag.*, vol. 49, no. 5, pp. 56–62, May 2011.

[9] H. Hashemi, "The indoor radio propagation channel," *Proc. IEEE*, vol. 81, no. 7, pp. 943–968, Jul. 1993.

[10] J.-F. Lemieux, M. El-Tanany, and H. Hafez, "Experimental evaluation of space/frequency/polarization diversity in the indoor wireless channel," *IEEE Trans. Veh. Technol.*, vol. 40, no. 3, pp. 569–574, Aug. 1991.

[11] J. B. Andersen, T. S. Rappaport, and S. Yoshida, "Propagation measurements and models for wireless communications channels," *IEEE Commun. Mag.*, vol. 33, no. 1, pp. 42–49, Jan. 1995.

[12] F. van der Wijk, A. Kegel, and R. Prasad, "Assessment of a pico-cellular system using propagation measurements at 1.9 GHz for indoor wireless communications," *IEEE Trans. Veh. Technol.*, vol. 44, no. 1, pp. 155–162, Feb. 1995.

[13] I. Khan and P. S. Hall, "Experimental evaluation of MIMO capacity and correlation for narrowband body-centric wireless channels," *IEEE Trans. Antennas Propag.*, vol. 58, no. 1, pp. 195–202, Jan. 2010.

[14] Q. Spencer, B. Jeffs, M. Jensen, and A. Swindlehurst, "Modeling the statistical time and angle of arrival characteristics of an indoor multipath channel," *IEEE J. Sel. Areas Commun.*, vol. 18, no. 3, pp. 347–360, Mar. 2000.

[15] M. Z. Win and R. A. Scholtz, "On the energy capture of ultra-wide bandwidth signals in dense multipath environments," *IEEE Commun. Lett.*, vol. 2, no. 9, pp. 245–247, Sep. 1998.

[16] ——, "On the robustness of ultra-wide bandwidth signals in dense multipath environments," *IEEE Commun. Lett.*, vol. 2, no. 2, pp. 51–53, Feb. 1998.

[17] R. J.-M. Cramer, R. A. Scholtz, and M. Z. Win, "An evaluation of the ultra-wideband propagation channel," *IEEE Trans. Antennas Propag.*, vol. 50, no. 5, pp. 561–570, May 2002.

[18] D. Cassioli, M. Z. Win, and A. F. Molisch, "The ultra-wide bandwidth indoor channel: From statistical model to simulations," *IEEE J. Sel. Areas Commun.*, vol. 20, no. 6, pp. 1247–1257, Aug. 2002.

[19] M. Z. Win and R. A. Scholtz, "Characterization of ultra-wide bandwidth wireless indoor communications channel: A communication theoretic view," *IEEE J. Sel. Areas Commun.*, vol. 20, no. 9, pp. 1613–1627, Dec. 2002.

[20] A. F. Molisch, D. Cassioli, C.-C. Chong, S. Emami, A. Fort, B. Kannan, J. Karedal, J. Kunisch, H. Schantz, K. Siwiak, and M. Z. Win, "A comprehensive standardized model for ultrawideband propagation channels," *IEEE Trans. Antennas Propag.*, vol. 54, no. 11, pp. 3151–3166, Nov. 2006, special issue on *Wireless Communications*.

[21] C.-C. Chong and S. K. Yong, "A generic statistical-based UWB channel model for high-rise apartments," *IEEE Trans. Antennas Propag.*, vol. 53, pp. 2389–2399, 2005.

[22] A. F. Molisch, "Ultrawideband propagation channels-theory, measurement, and modeling," *IEEE Trans. Veh. Technol.*, vol. 54, no. 5, pp. 1528–1545, Sep. 2005.

[23] ——, "Ultra-wide-band propagation channels," *Proc. IEEE*, vol. 97, no. 2, pp. 353–371, Feb. 2009.

[24] M. Z. Win and R. A. Scholtz, "Impulse radio: How it works," *IEEE Commun. Lett.*, vol. 2, no. 2, pp. 36–38, Feb. 1998.

[25] ——, "Ultra-wide bandwidth time-hopping spread-spectrum impulse radio for wireless multiple-access communications," *IEEE Trans. Commun.*, vol. 48, no. 4, pp. 679–691, Apr. 2000.

[26] L. Yang and G. B. Giannakis, "Ultra-wideband communications: An idea whose time has come," *IEEE Signal Process. Mag.*, vol. 21, no. 6, pp. 26–54, Nov. 2004.

[27] Y. Shen and M. Z. Win, "On the accuracy of localization systems using wideband antenna arrays," *IEEE Trans. Commun.*, vol. 58, no. 1, pp. 270–280, Jan. 2010.

[28] ——, "Fundamental limits of wideband localization – Part I: A general framework," *IEEE Trans. Inf. Theory*, vol. 56, no. 10, pp. 4956–4980, Oct. 2010. [Online]. Available: http://arxiv.org/abs/1006.0888v1

[29] S. Gezici, Z. Tian, G. B. Giannakis, H. Kobayashi, A. F. Molisch, H. V. Poor, and Z. Sahinoglu, "Localization via ultra-wideband radios: a look at positioning aspects for future sensor networks," *IEEE Signal Process. Mag.*, vol. 22, no. 4, pp. 70–84, Jul. 2005.

[30] D. Dardari, E. Falletti, and M. Luise, *Satellite and Terrestrial Radio Positioning Techniques - A signal processing perspective.* Elsevier Ltd., London, 2011.

[31] R. J. Fontana and S. J. Gunderson, "Ultra-wideband precision asset location system," *Proc. IEEE Conf. on Ultra Wideband Syst. and Technol. (UWBST)*, vol. 21, no. 1, pp. 147–150, May 2002.

[32] D. B. Jourdan, D. Dardari, and M. Z. Win, "Position error bound for UWB localization in dense cluttered environments," *IEEE Trans. Aerosp. Electron. Syst.*, vol. 44, no. 2, pp. 613–628, Apr. 2008.

[33] L. Stoica, A. Rabbachin, and I. Oppermann, "A low-complexity noncoherent IR-UWB transceiver architecture with TOA estimation," *IEEE Trans. Microw. Theory Tech.*, vol. 54, no. 4, pp. 1637–1646, Jun. 2006.

[34] D. Dardari, "Pseudo-random active UWB reflectors for accurate ranging," *IEEE Commun. Lett.*, vol. 8, no. 10, pp. 608–610, Oct. 2004.

[35] Y. Qi, H. Kobayashi, and H. Suda, "Analysis of wireless geolocation in a non-line-of-sight environment," *IEEE Trans. Wireless Commun.*, vol. 5, no. 3, pp. 672–681, 2006.

[36] D. Dardari, C.-C. Chong, and M. Z. Win, "Threshold-based time-of-arrival estimators in UWB dense multipath channels," *IEEE Trans. Commun.*, vol. 56, no. 8, pp. 1366–1378, Aug. 2008.

[37] C. Falsi, D. Dardari, L. Mucchi, and M. Z. Win, "Time of arrival estimation for UWB localizers in realistic environments," *EURASIP J. Appl. Signal Process.*, vol. 2006, pp. Article ID 32 082, 1–13, 2006, special issue on *Wireless Location Technologies and Applications*.

[38] K. Yu and I. Oppermann, "Performance of UWB position estimation based on time-of-arrival measurements," in *Proc. Int. Workshop on Ultra Wideband Syst. (IWUWBS)*, Oulu, Finland, May 2004, pp. 400–404.

[39] D. Dardari, A. Conti, U. J. Ferner, A. Giorgetti, and M. Z. Win, "Ranging with ultrawide bandwidth signals in multipath environments," *Proc. IEEE*, vol. 97, no. 2, pp. 404–426, Feb. 2009.

[40] B. Alavi and K. Pahlavan, "Modeling of the TOA-based distance measurement error using UWB indoor radio measurements," *IEEE Commun. Lett.*, vol. 10, no. 4, pp. 275–277, Apr. 2006.

[41] Y. Shen and M. Z. Win, "Energy efficient location-aware networks," in *Proc. IEEE Int. Conf. on Commun.*, Beijing, China, May 2008, pp. 2995–3001.

[42] J. Schroeder, S. Galler, K. Kyamakya, and K. Jobmann, "NLOS detection algorithms for ultra-wideband localization," in *Workshop on Positioning, Navigation and Commun. (WPNC)*, Mar. 2007, pp. 159–166.

[43] J. Khodjaev, Y. Park, and A. S. Malik, "Survey on NLOS identification and error mitigation problems in UWB-based positioning algorithms for dense environments," in *Annals of Telecommunications*, 2009.

[44] J. Schroeder, S. Galler, K. Kyamakya, and T. Kaiser, "Three-dimensional indoor localization in non line of sight UWB channels," in *Proc. IEEE Int. Conf. on Ultra-Wideband (ICUWB)*, Singapore, Sep. 2007.

[45] S. Maranò, W. M. Gifford, H. Wymeersch, and M. Z. Win, "NLOS identification and mitigation for localization based on UWB experimental data," *IEEE J. Sel. Areas Commun.*, vol. 28, no. 7, pp. 1026–1035, Sep. 2010.

[46] H. Wymeersch, S. Maranò, W. M. Gifford, and M. Z. Win, "A machine learning approach to ranging error mitigation for UWB localization," *IEEE Trans. Commun.*, vol. 60, 2012, to appear.

[47] D. Dardari, A. Conti, J. Lien, and M. Z. Win, "The effect of cooperation on localization systems using UWB experimental data," *EURASIP J. Appl. Signal Process.*, vol. 2008, pp. Article ID 513 873, 1–11, 2008, special issue on *Cooperative Localization in Wireless Ad Hoc and Sensor Networks*.

[48] A. Muqaibel, A. Safaai-Jazi, A. Bayeam, A. M. Attiya, and S. M. Riad, "Ultrawideband through-the-wall propagation," *IEE Proc. Microw. Antennas Propag.*, vol. 152, no. 6, pp. 581–588, Dec. 2005.

[49] A. Rabbachin, I. Oppermann, and B. Denis, "ML time-of-arrival estimation based on low complexity UWB energy detection," in *Proc. IEEE Int. Conf. on Ultra-Wideband (ICUWB)*, Waltham, MA, Sep. 2006, pp. 599–604.

[50] I. Güvenç, C.-C. Chong, F. Watanabe, and H. Inamura, "NLOS identification and weighted least-squares localization for UWB systems using multipath channel statistics," *EURASIP J. Adv. in Signal Process.*, vol. 2008, pp. 1–14, 2008.

[51] M. Guerra and A. Conti, "Experimental multilevel NLOS characterization for UWB network localization," in *Proc. IEEE Workshop on Statistical Signal Process.*, Nice, France, Jun. 2011, pp. 28–30.

[52] H. Wymeersch, J. Lien, and M. Z. Win, "Cooperative localization in wireless networks," *Proc. IEEE*, vol. 97, no. 2, pp. 427–450, Feb. 2009.

[53] A. Conti, M. Z. Win, M. Chiani, and J. H. Winters, "Bit error outage for diversity reception in shadowing environment," *IEEE Commun. Lett.*, vol. 7, no. 1, pp. 15–17, Jan. 2003.

Andrea Conti (S'99-M'01-SM'11) is a Professore Aggregato at the University of Ferrara, Italy. His research interests involve theory and experimentation of wireless systems and networks including network localization, adaptive diversity communications, and cooperative relaying techniques. Dr. Conti is serving as an Editor for the IEEE COMMUNICATIONS LETTERS and IEEE WIRELESS COMMUNICATIONS LETTERS, and served as an Associate Editor for the IEEE TRANSACTIONS ON WIRELESS COMMUNICATIONS (2003-2009). He is elected Vice-Chair of the IEEE Communications Society's Radio Communications Technical Committee (2011-2012).

Matteo Guerra received the Laurea degree (*summa cum laude*) in electronics and telecommunications engineering from the University of Ferrara, Italy, in 2011. He is a Ph.D. candidate at the University of Ferrara. His research interests include network localization and navigation. Mr. Guerra served in the local organization committee of the IEEE ICUWB 2011.

Davide Dardari (M'95-SM'07) is an Associate Professor at the University of Bologna at Cesena, Italy. His research interests are in ultrawide bandwidth communication and localization, wireless sensor networks, and OFDM systems. Dr. Dardari is serving as an Associate Editor for the IEEE TRANSACTIONS ON WIRELESS COMMUNICATIONS. He is elected Chair of the IEEE Communications Society's Radio Communications Technical Committee (2011-2012). He is a recipient of IEEE Aerospace and Electronic Systems Societys M. Barry Carlton Award.

Nicolò Decarli (S'10) received the Laurea degree (*summa cum laude*) in telecommunications engineering from the University of Bologna, Italy, in 2009. He is a Ph.D. candidate at the University of Bologna. His research interests include wireless communications and signal processing. His current research focuses on ultra-wide bandwidth communications and wideband localization. Mr. Decarli served in the local organization committee of IEEE ICUWB 2011.

Moe Z. Win (S'85-M'87-SM'97-F'04) is an Associate Professor at the Massachusetts Institute of Technology and the founding director of the Wireless Communication and Network Sciences Laboratory. His research encompasses developing fundamental theories, designing algorithms, and conducting experimentation for a broad range of real-world problems. Dr. Win is an elected Member-at-Large on the IEEE Communications Society Board of Governors (2011-2013). He received the Copernicus Fellowship and Laurea Honoris Causa from the University of Ferrara. He is elected Fellow of AAAS and IEEE, and recipient of the IEEE Kiyo Tomiyasu Award and the IEEE Eric E. Sumner Award.